Physica E 48 (2013) 101–105

Contents lists available at SciVerse ScienceDirect

Physica E

journal homepage: www.elsevier.com/locate/physe

Sign-changeable spin-filter efficiency in linear carbon atomic chain

Jiaxin Zheng [a,b,1], Chengyong Xu [a,1], Lu Wang [c], Qiye Zheng [a], Hong Li [a], Qihang Liu [a], Ruge Quhe [a], Zhengxiang Gao [a], Junjie Shi [a], Jing Lu [a,*]

[a] State Key Laboratory of Mesoscopic Physics and Department of Physics, Peking University, Beijing 100871, PR China
[b] Academy for Advanced Interdisciplinary Studies, Peking University, Beijing 100871, PR China
[c] Department of Physics, University of Nebraska at Omaha, Omaha, Nebraska 68182-0266, USA

HIGHLIGHTS

- We examine for the first time the quantum transport properties of a linear carbon atomic chain connected to two half-planar graphene electrodes at finite bias by using the first-principle method.
- We reveal that sign of the SFE of such carbon atomic chain is changeable with the bias.
- This property makes carbon atomic chains attractive to potential application of spintronic logic circuit.

ARTICLE INFO

Article history:
Received 8 September 2012
Received in revised form
15 November 2012
Accepted 14 December 2012
Available online 26 December 2012

ABSTRACT

It is well known that there is spin-filter efficiency (SFE) of a linear carbon atomic chain. In this article, we examine the quantum transport calculations of a linear carbon atomic chain connected to two half-planar graphene electrodes by using the first-principle method and reveal for the first time that sign of the SFE of such carbon atomic chain is changeable with the bias. This makes the carbon atomic chains attractive to potential application of spintronics.

1. Introduction

Due to the remarkable long spin relaxation time and length [1–5], carbon-based nanodevices are expected to be a promising candidate in nano spintronics. Recently, carbon nanodevices have been fabricated experimentally [6,7], showing excellent transport properties. Motivated by the aim to reduce the size of carbon devices, carbon atomic chains, which have been fabricated experimentally, were taken into consideration. By using the chemical method, compound of carbon chains attached by various chemical functional groups are obtained [8–12]. Pristine carbon chains can also be obtained by using the physical method: carbon chains are first prepared by hydrogen arc discharge and then inserted inside multi-walled carbon nanotubes [13]. Electron beam irradiation cuts single layer graphene to narrow nanoribbons or linear carbon atomic chains [14]. First principle calculations [14,15] help to verify the stability of carbon chains and find that the average bond length of carbons on the chains is smaller than that of the graphene nanoribbon edges [14].

It is important to understand the transport properties of the ultimate carbon nanodevices consisting of a single carbon atom chain. Theoretical studies have been made employing density functional theory combined with the nonequilibrium Green's function [15–21] or scattering-state formalisms [22–25]. Electronic [15,19,22,26] and magnetic [15,26] properties of individual carbon atomic chains [22,26] or chains between metallic electrodes [15,19–21] have been investigated to explain the transport phenomena. Carbon atomic chains connected to capped carbon nanotubes were found to exhibit negative differential resistance [12,20]. Taking advantage of the magnetic properties of carbon atomic chains, spin polarization is predicted when carbon chains are inserted between Au [15,27], graphene nanoribbons [21,28], and graphene plane [29] electrodes. Among these two-probe models of a carbon atomic chain, the carbon atomic chain connecting to graphene is the only realistic structure. However, the spin-polarized transport of this model has been investigated only at zero bias. As the transmission values near the Fermi level (E_f) at zero bias are extremely low, no more than 10^{-4}, little is known in this case. Further calculation at finite bias is required to understand the transport properties of carbon chains in detail. Meanwhile, a device functions at finite bias, and a check of the transport at finite bias is of actual importance.

In this article, we perform first-principle quantum transport calculation of finite linear carbon atomic chains connected to half-

* Corresponding author.
E-mail address: jinglu@pku.edu.cn (J. Lu).
[1] These authors contributed equally to this work.

1386-9477/$ - see front matter © 2012 Elsevier B.V. All rights reserved.
http://dx.doi.org/10.1016/j.physe.2012.12.009

planar graphene layers, a structure realized by Jin et al. [14], with respect to bias. For all the checked linear carbon atomic chains, we find that the devices are spin-polarized at finite bias. The spin-filter efficiency (SFE) is very large (up to 90% in magnitude) at certain bias. Most impressively, the sign of SFE changing with respect to the bias is observed, which is important in spintronic logic circuits.

2. Model and method

The two-probe model, shown in Fig. 1(a), consists of a linear carbon atomic chain contacted by semi-planar graphene layers. A carbon chain is denoted by C_N, where N is the number of carbon atoms on the chain. The examined carbon chains have atoms of $N=7$–12 with length $l=6.5$–14.3 Å. As shown in Fig. 1(b), the carbon atoms on the chain are labeled as from $C_{(1)}$ to $C_{(N)}$, and the atom in graphene attached to the left (right) end of the chain is referred to as $C_{(L)}$ ($C_{(R)}$). The inter-atomic distance along the chain is denoted by d_n ($0 \le n \le N$) as shown in Fig. 1(b), and each is set as 1.3 Å before geometric relaxation according to previous ab initio calculations [14,15]. The separation distance between two neighboring carbon chains in the same plane is 12.3 Å, and between two adjacent planes is 10.0 Å. The graphene edges are terminated with hydrogen atoms to remove additional dangling bonds. The carbon atoms on the chain are not passivated by other atoms, since they can form polyyne (C≡C–C≡C) or cumulene (C=C=C=C) [22,26,30–33] where no dangling bonds exist.

Based on the single-zeta basis set, geometric optimization and spin-unrestricted transport calculation are performed by using density functional theory (DFT) with the GGA-PBE exchange correlation functional as implemented in the Atomistix ToolKit 11.2 (ATK) package [17,34,35]. The devices are relaxed until the maximum force on each atom is less than 0.02 eV/Å. The k-points of integration over the first Brillouin zone are sampled at a $1 \times 10 \times 100$ [36] mesh. The electrode temperature is set at 300 K.

The spin-resolved current I_σ under the bias V_{bias} is calculated with the Landauer–Büttiker formula [37]:

$$I_\sigma(V_{bias}) = \frac{e}{h}\int_{-\infty}^{\infty} T_\sigma(E,V_{bias})[f_L(E,V_{bias}) - f_R(E,V_{bias})]dE, \quad (1)$$

where $T_\sigma(E, V_{bias})$ is the spin-polarized transmission probability, $f_{L/R}(E, V_{bias})$ the Fermi–Dirac distribution function of the left (L)/right (R) electrode, and σ the spin.

SFE at a finite bias is defined as:

$$SFE = \frac{I_{up} - I_{down}}{I_{up} + I_{down}}, \quad (2)$$

where I_{up} (I_{down}) is the spin-up (spin-down) current at the bias.

3. Results and discussion

The optimized inter-atomic distances for the C_7 and C_8 chains are given in Fig. 2, while those for other chains are provided in Supporting Information. It is obvious that the distances are symmetric with respect to the center of each carbon chain due to the symmetry of structure. The d_0 and d_n ($n=N+1$ for C_N chain) represent the distance between the graphene edge and the carbon chain. Varying from 1.38 to 1.41 Å according to different chains,

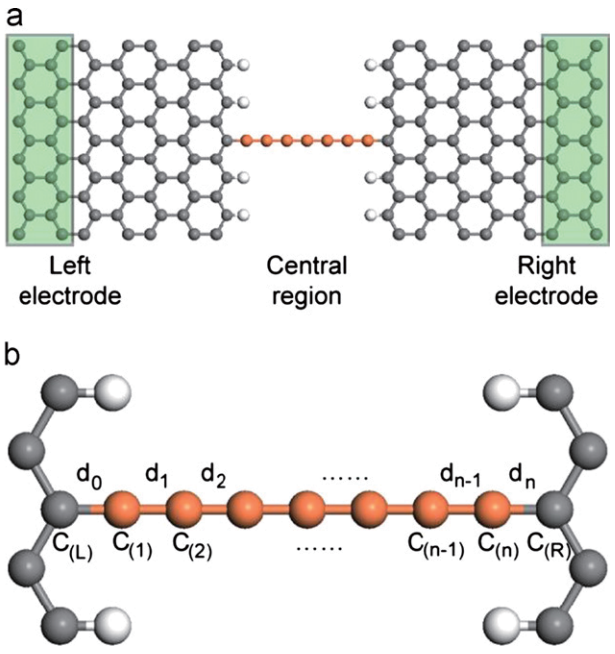

Fig. 1. (a) Schematic model of the C_7 chain connected to two semi-infinite graphene sheets. The green shaded area represents the electrodes. (b) Denotation of the carbon atoms and inter-atomic distance between neighboring carbon atoms along the chain. The orange, gray and, white balls denote the carbon atoms of the chain, of the graphene, and hydrogen atoms, respectively. (For interpretation of the references to color in this figure legend, the reader is referred to the web version of this article.)

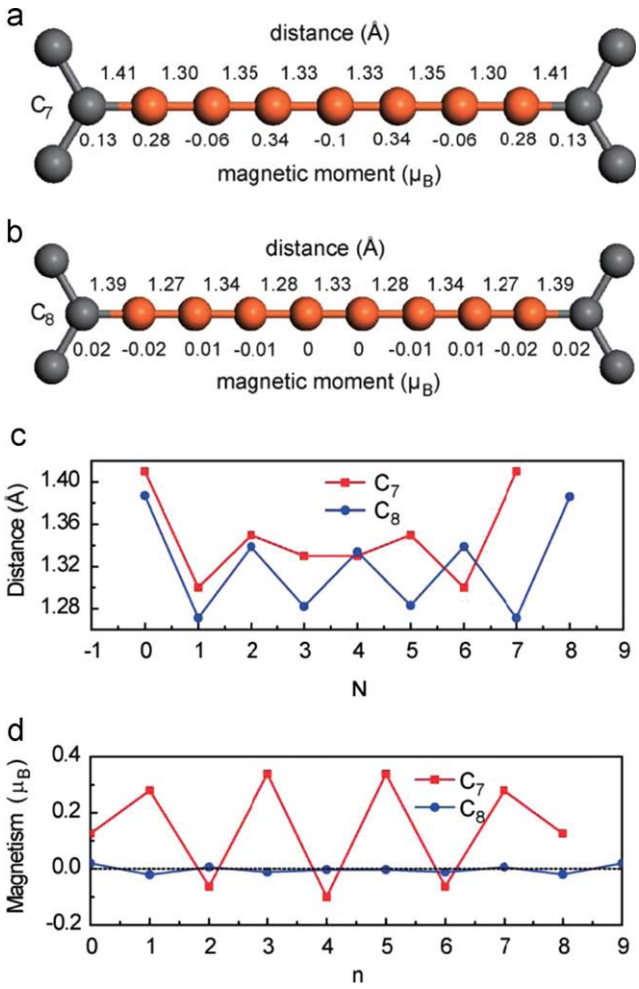

Fig. 2. Inter-atomic distances and magnetic moments of the (a) C_7 and (b) C_8 chains. Contrast of (c) the inter-atomic distances and (d) the magnetic moments of the C_7 and (b) C_8 chains.

d_0 and d_n are remarkably larger than other inter-atomic distances. It results from the fact that $C_{(L)}$ and $C_{(R)}$ are sp^2 hybridized like other atoms in graphene and that d_0 and d_n are close to the inter-atomic distance of 1.42 Å in graphene, suggesting longer $C_{(L)}$–$C_{(1)}$ and $C_{(N)}$–$C_{(R)}$ single bonding.

However, the atoms on the chains are sp hybridized, in this way $C_{(1)}$ and $C_{(2)}$ ($C_{(N-1)}$ and $C_{(N)}$) form into the shortest triple bonding $C_{(1)}\equiv C_{(2)}$ ($C_{(N-1)}\equiv C_{(N)}$), corresponding to the smallest d_1 (d_N). So is the case for d_2 and d_{N-1}. The behavior of the rest inter-atomic distances on each chain depends on whether the chain consists of odd or even atoms. For the even-numbered chains, there are odd inter-atomic intervals between neighboring atoms to accommodate alternatively single and triple bonds, therefore d_n oscillates with respect to n. However, the alternation of single and triple bonds does not hold for the odd-numbered chains. Instead, double bonds are formed. In this case, d_n decays from two ends to the center for each odd-numbered chain. In the very middle it is 1.31 to 1.33 Å, in well agreement with the C=C bond length(1.33 Å) of C_2H_4 i. The inter-atomic distances character mentioned above are in accord with those calculated by Li et al. [15] (the carbon chains are freestanding) and Zanolli et al. (the carbon atomic chains are contacted by two zigzag or armchair graphene nanoribbons) [28], because the bonding mechanism is the same.

Apart from the inter-atomic distances, the magnetic moments of the C_7 and C_8 carbon chains are displayed for in Fig. 2 and those of other carbon chains are shown in Supporting Information. The odd-numbered and even-numbered chains have different atomic magnetic moments. For the odd-numbered chains, the magnetic moments oscillate with respect to the atomic sequence, and the total magnetic moments are 1.2–1.3 μ_B. The magnetic moments of the C_7 chains on $C_{(L)}$ and $C_{(R)}$ are both 0.13 μ_B, on the odd-labeled atoms are higher, varying between 0.28 to 0.34 μ_B, and on the even-labeled atoms are no more than 0.1 μ_B. The different magnetic moments on the odd-labeled atoms of the C_7 chain indicate that the $C_{(L)}$, $C_{(R)}$ and odd-labeled atoms are not fully covalently bonded, while the even-labeled atoms are fully bonded. All the atoms along the C_8 chain are fully bonded as the magnetic moments on them are extremely small, being negligibly no more than 0.02 μ_B as shown in Fig. 2, and the total magnetic moments are zero. The magnetic moments of other chains respectively resemble those of the C_7 and C_8 chains, depending on whether they are odd- or even-numbered. The magnetic results of our devices are in accord with those of carbon

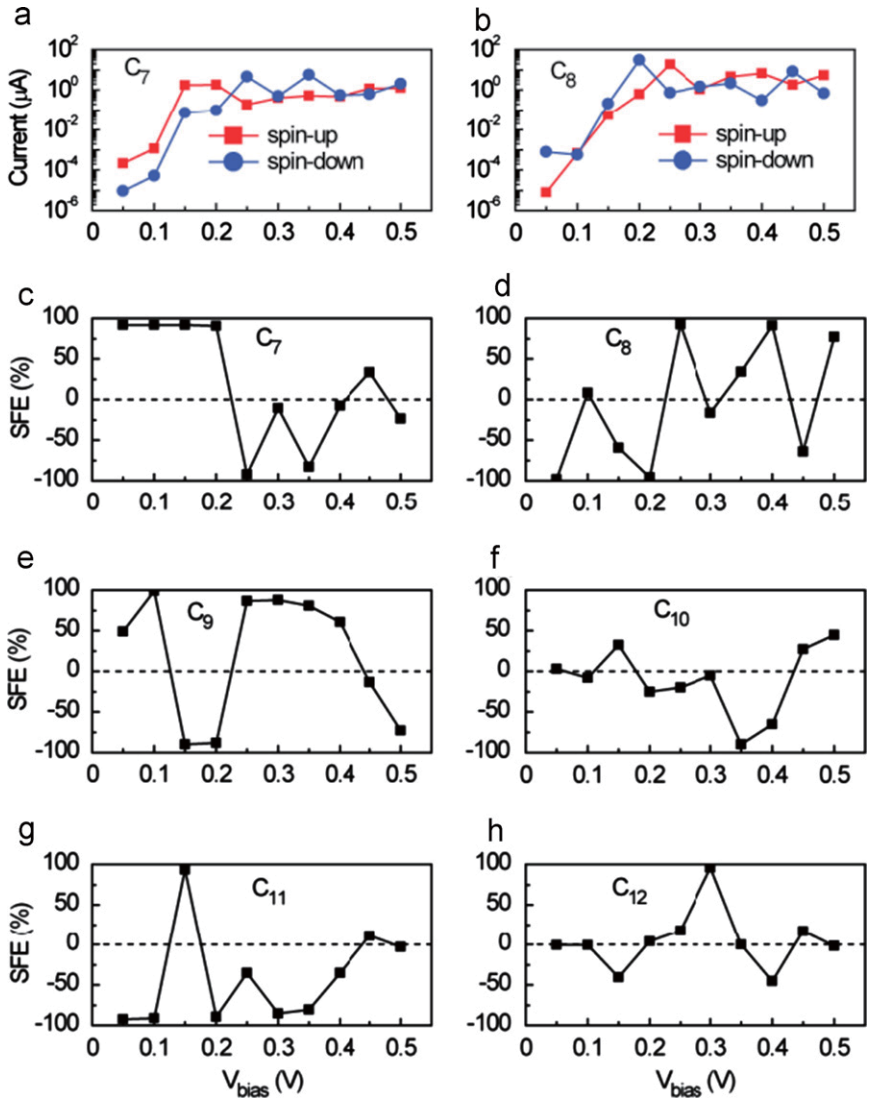

Fig. 3. Spin-polarized I–V_{bias} characteristics of the (a) C_7 and (b) C_8 chains. (c)–(h) SFE of each chain as a function of the bias.

chains connected to zigzag graphene nanoribbons [28]. However, they are contrary to those of freestanding carbon chains [15]. Freestanding odd-numbered carbon chains form into uniform double bonds, leaving no unpaired states, so that the total magnetic moments are zero. When these odd-numbered carbon chains are bonded to $C_{(L)}$ or $C_{(R)}$, the uniform double bonds are destroyed and the total magnetic moments are changed to 1.2–1.3 μ_B. Freestanding even-numbered carbon chains form into alternatively triple and single bonds, leaving an unsaturated state on two terminal atoms to accommodate two unpaired electrons, bring forth to total magnetic moments of 2.0 μ_B. When these two unoccupied states are removed by additional bonding of the even-numbered chain with $C_{(L)}$ or $C_{(R)}$, the total magnetic moments are changed to nearly zero.

The transport currents of all chains are spin-polarized, as displayed in Fig. 3(a) and (b) for the C_7 and C_8 chains and in Supporting Information for other chains. The SFEs of all chains are plotted in Fig. 3(c)–(h). We take the C_7 chain as an example to elucidate the currents and SFE. In the case of the C_7 chain, the spin-up currents at a bias lower than 0.2 V are much larger than the spin-down currents, resulting in very large positive SFEs (~91%). At a bias larger than 0.2 V (except 0.45 V), the spin-up currents are smaller than the spin-down currents, causing negative SFEs. This indicates that spin-polarization of the current can be controlled by increasing the bias voltage without resorting to magnetic field. Such sign-changeable of SFE is also observed for the other chains (Fig. 3). Sign-changeable of SFE was for the first time found in Fe/GaAs(0 0 1) interfaces [38,39] and earlier theoretical studies [40]. It is also found on the devices constructed from organometallic chains. This sign-changeable effect of SFE is important and of great potential for spintronic logic applications [41], where the spin signal is monitored by the bias voltage.

We investigate the transmission spectrum and the transmission eigenstates of the carbon chains. As the current is expressed

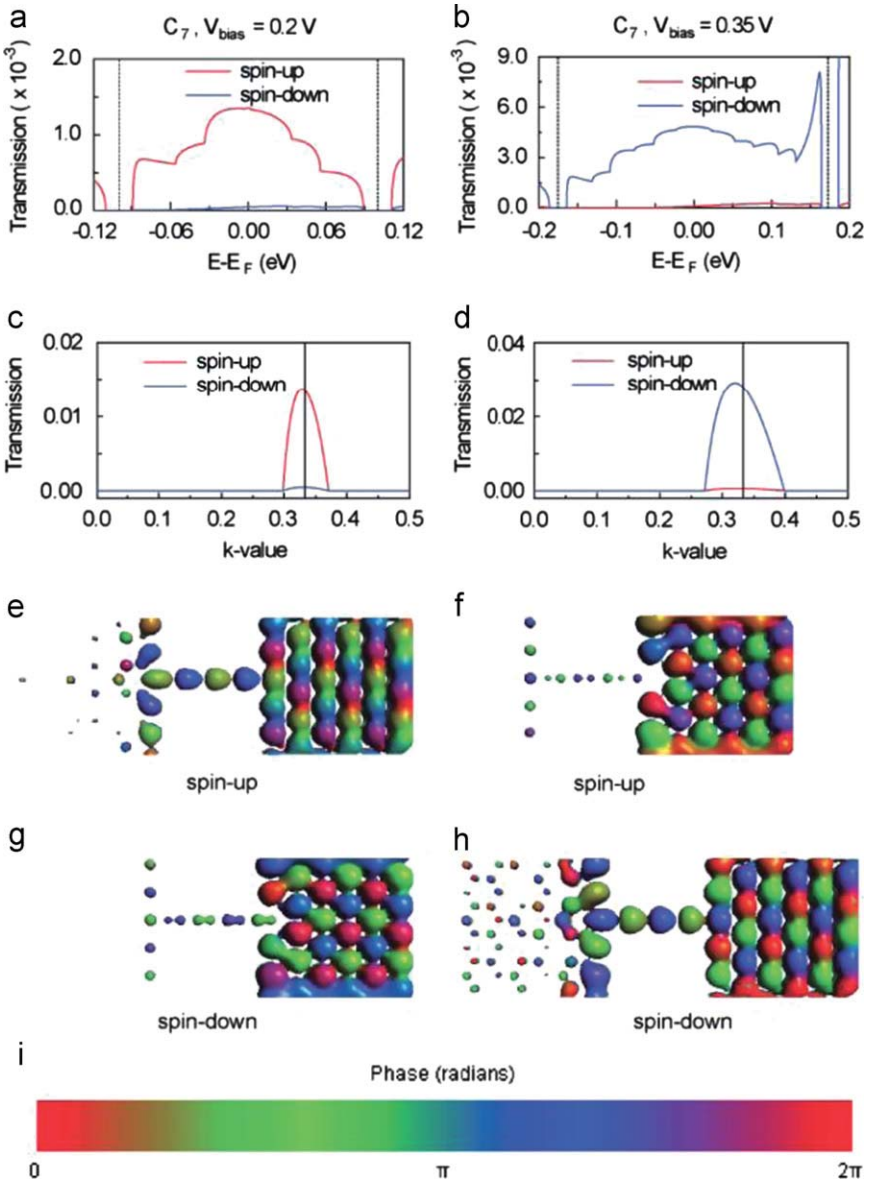

Fig. 4. (a–h) Transmission spectra and spin-resolved transmission eigenstates from the right region (those from the left region are shown in Fig. S4) of the C_7 chain device at V_{bias}=0.2 V (left panel) and V_{bias}=0.35 V (right panel). (a), (b) Transmission coefficients as a function of energy. The dashed vertical line indicates the bias window. (c), (d) Transmission as a function of k at E_f. (e), (f) Spin-up and (f)–(h) spin-down transmission eigenchannels at E_f and at $k_y = \pi/3a$. The isovalues of (e)–(h) are all 0.04 a.u. (i) Color bar of phase of eigenstates. (For interpretation of the references to color in this figure legend, the reader is referred to the web version of this article.)

as an integral of transmission spectrum together with the Fermi–Dirac distribution function, SFE is reflected in the contrast between the spin-up and spin-down transmission spectra. Taking the C_7 chain as an example, it is obvious that the transmission coefficients of up-spin are much larger than those of down-spin within the bias windows at $V_{bias}=0.2$ V (Fig. 4(a)), while the transmission coefficients of down-spin are larger than those of up-spin at $V_{bias}=0.35$ V (Fig. 4(b)). The transmission coefficients at E_f as a function of k_y value are shown in Fig. 4(c) and (d),and similar contrasts between the two spins at $V_{bias}=0.2$ and 0.35 V are available.

We show the transmission eigenchannels of the right region contribution at E_f and at $k_y=\pi/3a$ in Fig. 4(e)–(h). The transmission eigenchannels of the left region contribution is provided in Fig. S4. At $V_{bias}=0.2$ V, the transmission of spin-up electrons (Fig. 4(c)) is apparently stronger than that of spin-down electrons. The dominance of spin-up electrons over spin-down electrons is consistent with a large positive SFE (91%) at this bias. At $V_{bias}=0.35$ V, an opposite dominance of spin-down over spin-up electrons appears, in agreement with a large negative SFE (-83%) at this bias. The change of dominance reveals the sign-change of SFE from being positive to negative, which will be important in logic circuits.

Finally, in our model, if the carbon chain contains only one C atom, the spin of the single C atom will be coupled with the conduction electron spin and form a Kondo (spin-singlet) state, and both the DFT and the spin-filter function are invalidated. Therefore, in order to make the C chain work as a spin-filter, the chain should be enough long. So far the critical size at which the C chain behaves like an impurity is unknown, and additional work is expected to determine it. In our work, the smallest size is C_7 chain, which appears not too short. Anyway, a longer C chain is better for the sake of spin-filter function and escape from the Kondo state.

4. Conclusions

In summary, we have performed first-principle quantum transport calculations for linear carbon atomic chains connected to two graphene layers. All the checked carbon chains show very large SFE ($>90\%$ in magnitude) at certain bias voltage. SFE of each chain changes its sign with respect to the bias voltage. Therefore, the carbon atomic chains have potential application in spintronics.

Acknowledgment

This work was supported by the National Natural Science Foundation of China (Nos. 11274016, 51072007, 91021017, 11047018, and 60890193), the National Basic Research Program of China (Nos. 2013CB932604 and 2012CB619304), National 973 Projects (Nos. 2007CB936200 and 2006CB921607, MOST of China), Fundamental Research Funds for the Central Universities, National Foundation for Fostering Talents of Basic Science (No. J1030310/No.J1103205), and Program for New Century Excellent Talents in University of MOE of China.

Appendix A. Supporting information

Supplementary data associated with this article can be found in the online version at http://dx.doi.org/10.1016/j.physe.2012.12.009.

References

[1] C. Berger, Z.M. Song, T.B. Li, X.B. Li, A.Y. Ogbazghi, R. Feng, Z.T. Dai, A.N. Marchenkov, E.H. Conrad, P.N. First, W.A. de Heer, The Journal of Physical Chemistry B 108 (2004) 19912.
[2] K.S. Novoselov, A.K. Geim, S.V. Morozov, D. Jiang, Y. Zhang, S.V. Dubonos, I.V. Grigorieva, A.A. Firsov, Science 306 (2004) 666.
[3] K.S. Novoselov, A.K. Geim, S.V. Morozov, D. Jiang, M.I. Katsnelson, I.V. Grigorieva, S.V. Dubonos, A.A. Firsov, Nature 438 (2005) 197.
[4] C. Berger, Z.M. Song, X.B. Li, X.S. Wu, N. Brown, C. Naud, D. Mayou, T.B. Li, J. Hass, A.N. Marchenkov, E.H. Conrad, P.N. First, W.A. de Heer, Science 312 (2006) 1191.
[5] A.K. Geim, K.S. Novoselov, Nature Materials 6 (2007) 183.
[6] M.C. Lemme, T.J. Echtermeyer, M. Baus, H. Kurz, IEEE Electron Device Letters 28 (2007) 282.
[7] X. Liang, Z. Fu, S.Y. Chou, Nano Letters 7 (2007) 3840.
[8] J.R. Heath, Q. Zhang, S.C. Obrien, R.F. Curl, H.W. Kroto, R.E. Smalley, Journal of the American Chemical Society 109 (1987) 359.
[9] R.J. Lagow, J.J. Kampa, H.C. Wei, S.L. Battle, J.W. Genge, D.A. Laude, C.J. Harper, R. Bau, R.C. Stevens, J.F. Haw, E. Munson, Science 267 (1995) 362.
[10] V. Derycke, P. Soukiassian, A. Mayne, G. Dujardin, J. Gautier, Physical Review Letters 81 (1998) 5868.
[11] H.E. Troiani, M. Miki-Yoshida, G.A. Camacho-Bragado, M.A.L. Marques, A. Rubio, J.A. Ascencio, M. Jose-Yacaman, Nano Letters 3 (2003) 751.
[12] T.D. Yuzvinsky, W. Mickelson, S. Aloni, G.E. Begtrup, A. Kis, A. Zettl, Nano Letters 6 (2006) 2718.
[13] X.L. Zhao, Y. Ando, Y. Liu, M. Jinno, T. Suzuki, Physical Review Letters 90 (2003) 187401.
[14] C.H. Jin, H.P. Lan, L.M. Peng, K. Suenaga, S. Iijima, Physical Review Letters 102 (2009) 205501.
[15] Z.Y. Li, W. Sheng, Z.Y. Ning, Z.H. Zhang, Z.Q. Yang, H. Guo, Physical Review B 80 (2009) 115429.
[16] J. Taylor, H. Guo, J. Wang, Physical Review B 63 (2001) 245407.
[17] M. Brandbyge, J.L. Mozos, P. Ordejon, J. Taylor, K. Stokbro, Physical Review B 65 (2002) 165401.
[18] Y.Q. Xue, S. Datta, M.A. Ratner, Chemical physics 281 (2002) 151.
[19] R. Pati, M. Mailman, L. Senapati, P.M. Ajayan, S.D. Mahanti, S.K. Nayak, Physical Review B 68 (2003) 014412.
[20] K.H. Khoo, J.B. Neaton, Y.W. Son, M.L. Cohen, S.G. Louie, Nano Letters 8 (2008) 2900.
[21] M.G. Zeng, L. Shen, Y.Q. Cai, Z.D. Sha, Y.P. Feng, Applied Physics Letters 96 (2010) 042104.
[22] N.D. Lang, P. Avouris, Physical Review Letters 81 (1998) 3515.
[23] M. Di Ventra, N.D. Lang, Physical Review B 65 (2002) 045402.
[24] Y. Fujimoto, K. Hirose, Physical Review B 67 (2003) 195315.
[25] H.J. Choi, M.L. Cohen, S.G. Louie, Physical Review B 76 (2007) 155420.
[26] N.D. Lang, P. Avouris, Physical Review Letters 84 (2000) 358.
[27] Y. Wei, Y. Xu, J. Wang, H. Guo, Physical Review B 70 (2004) 193406.
[28] Z. Zanolli, G. Onida, J.-C. Charlier, ACS Nano 4 (2010) 5174.
[29] J.A. Fürst, M. Brandbyge, A.-P. Jauho, Europhysics letters 91 (2010) 37002.
[30] B. Larade, J. Taylor, H. Mehrez, H. Guo, Physical Review B 64 (2001) 075420.
[31] S. Tongay, R.T. Senger, S. Dag, S. Ciraci, Physical Review Letters 93 (2004) 4.
[32] Z. Crljen, G. Baranovicacute, Physical Review Letters 98 (2007) 116801.
[33] S. Okano, D. Tomanek, Physical Review B 75 (2007) 195409.
[34] ATOMISTIX Toolkit Version 11.08, QuantumWise A/S, 〈www.quantumwise.com〉.
[35] J. Taylor, H. Guo, J. Wang, Physical Review B 63 (2001) 245407.
[36] H.J. Monkhorst, J.D. Pack, Physical Review B 13 (1976) 5188.
[37] S. Datta, Electronic Transport in Mesoscopic Systems, Cambridge University Press, Cambridge, England, 1995.
[38] S.A. Crooker, M. Furis, X. Lou, C. Adelmann, D.L. Smith, C.J. Palmstrom, P.A. Crowell, Science 309 (2005) 2191.
[39] X.H. Lou, C. Adelmann, S.A. Crooker, E.S. Garlid, J.J. Zhang, K.S.M. Reddy, S.D. Flexner, C.J. Palmstrom, P.A. Crowell, Nature Physics 3 (2007) 197.
[40] A.N. Chantis, K.D. Belashchenko, D.L. Smith, E.Y. Tsymbal, M. van Schilfgaarde, R.C. Albers, Physical Review Letters 99 (2007) 196603.
[41] L. Wang, X.F. Gao, X. Yan, J. Zhou, Z.X. Gao, S. Nagase, S. Sanvito, Y. Maeda, T. Akasaka, W.N. Mei, J. Lu, Journal of Physical Chemistry C 114 (2010) 21893.